DALTON

Stabilization of copper(III) complexes by disubstituted oxamides and related ligands

Rafael Ruiz,[a] Céline Surville-Barland,[a] Ally Aukauloo,[a] Elodie Anxolabehere-Mallart,[a] Yves Journaux,*[,a] Joan Cano[b] and M. Carmen Muñoz[c]

[a] *Laboratoire de Chimie Inorganique, URA 420, CNRS, Université de Paris-Sud, 91405 Orsay, France*
[b] *Departament de Química Inorgànica, Universitat de València, Dr. Moliner 50, 46100 Burjassot, València, Spain*
[c] *Departamento de Física Aplicada, Universidad Politécnica de València, Camino de vera s/n, 46071 València, Spain*

The electrochemical behaviour of a family of monomeric copper(II) complexes of the related tetraanionic chelating ligands *N*,*N*′-*o*-phenylenebis(oxamate) (L^1) and its methylamide (L^2) and bis(methylamide) (L^3) has been investigated by cyclic voltammetry in acetonitrile at 25 °C and 0.1 mol dm^{-3} NEt_4ClO_4 as supporting electrolyte. The copper(III)–copper(II) reduction potentials have been found to span a potential range from +0.41 to −0.02 V (*vs.* saturated calomel electrode), being reversible for all cases except the copper(II)–L^1 complex. The trend in formal potentials along this series is explained in terms of the stronger donor properties of the deprotonated-amido nitrogen atoms than those of the carboxylate oxygen ones. Hence, the stabilization of the trivalent oxidation state of copper is attributed to the increasing number of deprotonated-amido donor groups. A perfect correlation has been observed within this family between the Cu^{III}–Cu^{II} potentials and the visible absorption maxima of the copper(II) complexes. The relative gain in crystal-field stabilization energy for the change from the d^9 (Cu^{II}, square planar) to the low-spin d^8 (Cu^{III}, square-planar) electronic configuration is the main factor in the overall thermodynamic stability of the copper(III) complexes. The molecular structure of the stable copper(III) complex $[PPh_4][CuL^3]\cdot MeCN$ has been determined by single-crystal X-ray analysis. The metal is in a nearly square-planar environment formed by the four amido nitrogen atoms of the chelating ligand, with short Cu–N bond distances (1.84–1.88 Å) typical of trivalent copper.

The co-ordination chemistry of high-oxidation-state transition-metal complexes is an area of considerable importance, because of their biological significance as models of redox enzymes and their potentially useful properties as catalytic oxidants, although limited in scope owing to the small number of suitable ligands.[1–3] One of them is the well known oxamide dianion $C_2O_2N_2H_2^{2-}$ which acting as a bidentate ligand through its strong electron-donating amide nitrogen atoms is able to stabilize high oxidation states, as has been shown by Steggerda and co-workers[4] for copper(III) and nickel(III). However, the low solubility of oxamide in common solvents and its weak acidity, together with its hydrolytic decomposition in alkaline solution, preclude an exhaustive exploration of its co-ordination chemistry. These difficulties can be almost overcome by using *N*,*N*′-bis(co-ordinating group-substituted)oxamides,[5] which are more reluctant to undergo hydrolysis and exhibit higher solubility. Furthermore, in the presence of transition-metal ions and if the substituted oxamide can form five- or six-membered chelate rings, the amide deprotonates and co-ordinates simultaneously at low pH.[6,7] The ability of this class of ligands to stabilize high oxidation states has been recently demonstrated by Lloret and co-workers[7d] in an extensive study of copper chemistry with *N*,*N*′-bis(carboxylate-substituted)oxamides, studies which are at the foundations of the present work.

In this paper we explore the capacity of one specific family of tetraanionic chelating ligands, namely *N*,*N*′-*o*-phenylenebis(oxamate), its methylamide and bis(methylamide) derivatives, in the stabilization of copper(III) complexes. The trend in formal potentials of the copper(III)–copper(II) couples as the O-carboxylic atoms are systematically replaced by N-amido ones along this series is explained in the light of their different donor properties. The crystal and molecular structure of the copper(III) complex $[PPh_4][CuL^3]\cdot MeCN$ is also reported, which constitutes one of the few examples of structurally characterized copper compounds in the rare +III oxidation state.[8–14]

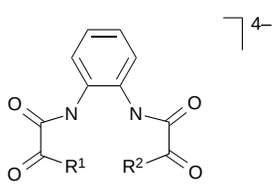

	R^1	R^2
L^1	O	O
L^2	O	NMe
L^3	NMe	NMe

Experimental

Materials

All chemicals were of reagent-grade quality from commercial sources and used as received, except those for electrochemical measurements. The NEt_4ClO_4 salt was recrystallized twice from acetone–diethyl ether and dried at 80 °C under vacuum. Acetonitrile was purified by distillation from calcium hydride on to activated 3 Å molecular sieves and stored under argon. The diethyl ester of *N*,*N*′-*o*-phenylenebis(oxamic acid) was prepared from ethyloxalyl chloride and *o*-phenylenediamine by literature methods.[15]

Preparations

H_4L^2 and H_4L^3. A methanolic solution (50 cm^3) of diethyl

N,*N*′-*o*-phenylenebis(oxamate) (10 mmol) was treated with either $\frac{2}{3}$ equivalent (for H_4L^2) or an excess, at least 3 equivalents (for H_4L^3), of methylamine (33% in ethanol) at room temperature. The mixture was kept at 65 °C for half an hour with vigorous stirring and the white precipitate was filtered off, washed with methanol and diethyl ether, and dried under vacuum (*ca.* 90%) (Found: C, 51.9; H, 4.8; N, 15.4. $C_{12}H_{13}N_3O_5$ requires C, 51.1; H, 4.7; N, 15.05%. Found: C, 52.0; H, 4.9; N, 20.2. $C_{12}H_{14}N_4O_4$ requires C, 51.8; H, 5.1; N, 20.1%). $\tilde{\nu}_{max}/cm^{-1}$ (KBr) 3259s (NH) and 1762vs, 1740vs and 1690vs (CO) for the diethyl ester; 3310s and 3263s (NH) and 1718s and 1657vs (CO) for H_4L^2; 3379s, 3323s and 3257s (NH) and 1690s and 1660vs (CO) for H_4L^3. $\delta_H[(CD_3)_2SO]$ 1.35 (6 H, t, 2 CH_3), 4.34 (4 H, q, 2 CH_2O), 7.24 (2 H, dd, *m*-H of C_6H_4), 7.56 (2 H, dd, *o*-H of C_6H_4) and 9.26 (2 H, s, 2 NH) for diethyl ester; 2.72 (3 H, d, CH_3N), 3.85 (3 H, s, CH_3O), 7.28 (2 H, dd, *m*-H of C_6H_4), 7.52 (1 H, dd, *o*-H of C_6H_4), 7.62 (1 H, dd, *o*-H of C_6H_4), 8.99 (1 H, d, NH alkyl), 10.36 (2 H, s, NH aryl) and 10.58 (2 H, s, NH aryl) for H_4L^2; 2.73 (6 H, d, 2 CH_3N), 7.29 (2 H, dd, *m*-H of C_6H_4), 7.60 (2 H, dd, *o*-H of C_6H_4), 8.99 (2 H, q, 2 NH alkyl) and 10.50 (2 H, s, 2 NH aryl) for H_4L^3.

$Na_2[CuL^1]\cdot 3H_2O$ 1, $Na_2[CuL^2]\cdot 2H_2O$ 2 and $Na_2[CuL^3]\cdot H_2O$ 3. The cuprate(II) salts **1**–**3** were synthesized by following a procedure analogous to that reported previously for **1**:[14] to a suspension of the corresponding oxamate (5 mmol) in water (250 cm^3) was added an aqueous solution (25 cm^3) of NaOH (1.00 g, 25 mmol). The mixture was stirred at 60 °C for 15 min. An aqueous solution (50 cm^3) of $Cu(ClO_4)_2\cdot 6H_2O$ (1.85 g, 5 mmol) was then added dropwise with stirring. The resulting mixture was charged with water until complete dissolution. It was then filtered, reduced to approximately half the initial volume on a rotatory evaporator when a solid began to appear. The powdered precipitate was filtered off, washed with ethanol and ether, and air-dried.

$[NMe_4]_2[CuL^1]\cdot H_2O$ 4, $[NMe_4]_2[CuL^2]\cdot H_2O$ 5 and $[NMe_4]_2[CuL^3]\cdot H_2O$ 6. The cuprate(II) salts **4**–**6** were prepared similarly: to a suspension of the corresponding oximate (5 mmol) in methanol (100 cm^3) was added a 25% methanol solution (10 cm^3) of NMe_4OH (25 mmol). The resulting mixture was stirred at 60 °C for 15 min until complete dissolution. A methanolic solution (50 cm^3) of $Cu(ClO_4)_2\cdot 6H_2O$ (1.85 g, 5 mmol) was then added dropwise with stirring. It was filtered to remove solid NMe_4ClO_4, reduced to *ca.* 10 cm^3 on a rotatory evaporator, and an equal volume of acetonitrile added to precipitate the remaining NMe_4ClO_4. The mixture was filtered again and treated successively with ether and acetone to give a hygroscopic solid which was rapidly filtered off and dried under vacuum.

$[PPh_4]_2[CuL^1]\cdot H_2O$ 7, $[PPh_4]_2[CuL^2]\cdot 4H_2O$ 8 and $[PPh_4]_2[CuL^3]\cdot 5H_2O$ 9. The cuprate(II) salts **7**–**9** were obtained by metathesis of the sodium salts **1**–**3**, respectively, with tetraphenylphosphonium chloride in water at room temperature as follows: PPh_4Cl (3.75 g, 10 mmol) dissolved in the minimum volume of water was added dropwise to a previously filtered aqueous solution of the corresponding sodium salt (5 mmol). A polycrystalline solid precipitated immediately, and was filtered off, washed with ethanol and ether, and air-dried.

$[PPh_4][CuL^3]\cdot MeCN$ 10. The copper(III) complex **10** was obtained by chemical oxidation of the corresponding copper(II) complex with iodine in dichloromethane as follows: to complex **9** (1.10 g, 1 mmol) dissolved in dichloromethane (50 cm^3) was added a dichloromethane solution containing a slight excess of I_2 (0.15 g, 0.6 mmol) with gentle warming. The intensely coloured solution was filtered and then allowed to evaporate slowly. Recrystallization from acetonitrile afforded the desired product as well shaped large prismatic brown-black crystals suitable for X-ray analysis, which were separated by hand from the residual PPh_4I. The compound exhibits unusual stability; for instance, no significant decomposition occurs during the recrystallization procedure even over several days.

Analytical and general physical characterization data for the copper compounds **1**–**10** are listed in Table 1.

Physical techniques

Proton NMR spectra were recorded at 250 MHz on a Brüker AC 250 spectrometer. Chemical shifts are reported in δ (ppm) *vs.* $SiMe_4$ with the deuteriated solvent proton residuals as internal standard. The ESR spectra were recorded on a Brüker ER 200 D spectrometer at X-band at 298 K, IR spectra on a Perkin-Elmer 882 spectrophotometer as KBr pellets and visible solution spectra on a Cary 1 UV/VIS spectrophotometer. Elemental analyses (C, H, N) were performed by the Microanalytical Service of Institut de Chimie des Substances Naturelles (Centre National de la Recherche Scientifique).

Cyclic voltammetry was performed using a Princeton Applied Research Model 362 scanning potentiostat. The electrochemical studies were carried out in acetonitrile using 0.1 mol dm^{-3} NEt_4ClO_4 as supporting electrolyte. The tetramethylammonium and tetraphenylphosphonium cuprate(II) salts (1.0 mmol dm^{-3}) gave identical results. The working electrode was a glassy carbon disc (0.32 cm^2) which was polished with 0.3 μm polishing powder, sonicated, washed with distilled water and acetone, and vacuum dried. The reference electrode was $Ag(AgClO_4)$ separated from the test solution by a salt bridge containing the solvent/supporting electrolyte, with platinum as auxiliary electrode. All experiments were performed in standard electrochemical cells under an inert atmosphere at 25 °C. All formal potentials were taken as the anodic peak potentials (E_p) and are referred to the saturated calomel electrode (SCE), which was consistently measured as −0.26 V *vs.* the $AgClO_4$–Ag electrode. The peak-to-peak separations (ΔE_p) of the copper couples, when both anodic and cathodic peaks were detected, were similar to that of the ferrocenium–ferrocene couple under the same conditions, *i.e.* around 50 mV. Plots of peak current *vs.* the square root of the scan rate over the range 50–200 mV s^{-1} were linear for couples that are stated to be reversible.

Crystallography

Crystal data and data collection parameters. $C_{38}H_{33}CuN_5O_4P$, $M = 718.24$, monoclinic, space group $P2_1/a$, $a = 10.847(2)$, $b = 22.081(4)$, $c = 14.898(4)$ Å, $\beta = 110.53(2)°$, $U = 3568$ $Å^3$ (by least-squares refinement on diffractometer angles from 25 centred reflections, $12 < \theta < 20°$), 293 K, graphite-monochromated Mo-Kα radiation, $\lambda = 0.710\,69$ Å, $Z = 4$, $D_c = 1.42$ g cm^{-3}, $F(000) = 1476$, brown-black prism with dimensions $0.25 \times 0.11 \times 0.08$ mm, $\mu(Mo\text{-}K\alpha) = 9.5$ cm^{-1}.

Corrections for Lorentz-polarization effects but not absorption were carried out (the latter was not considered necessary given the low μ value); Enraf-Nonius CAD-4 diffractometer, data collection range $1 \leqslant \theta \leqslant 25°$, three standard reflections monitored throughout data collection showed no significant variation in intensity; 6630 reflections measured, 4080 unique with $I \geqslant 3\sigma(I)$ used in all calculations.

Structure solution and refinement. The structure was solved by Patterson methods and refined by the full-matrix least-squares method on F^2. All non-hydrogen atoms were refined anisotropically. The hydrogen atoms were located from a difference synthesis and refined with an overall isotropic thermal parameter. The final full-matrix least-squares refinement, minimizing $\Sigma w(|F_o| - |F_c|)^2$ with unit weights, converged at $R = R' = 0.048$ $\{R = \Sigma(|F_o| - |F_c|)/\Sigma(|F_o|)$ and $R' = [\Sigma(|F_o| - |F_c|)^2/\Sigma wF_o^2]^{\frac{1}{2}}\}$, for 445 refined parameters, goodness of fit = 1.484, maximum $\Delta/\sigma = 0.1$, maximum $\Delta\rho = 1.569$ e $Å^{-3}$, minimum

Table 1 Analytical[a] and physical data for the copper complexes

Complex	Colour	$\tilde{\nu}$(CO)[b]/cm^{-1}	Yield (%)	Analysis (%) C	H	N
1 $Na_2[CuL^1]\cdot 3H_2O$	Violet	1643s, 1617vs	85	29.3 (29.2)	2.45 (2.45)	6.7 (6.8)
2 $Na_2[CuL^2]\cdot 2H_2O$	Pink	1610vs (br)	80	32.3 (32.5)	2.9 (2.7)	9.85 (10.3)
3 $Na_2[CuL^3]\cdot H_2O$	Red	1602vs (br), 1580s	80	35.5 (35.9)	3.2 (3.0)	13.6 (13.9)
4 $[NMe_4]_2[CuL^1]\cdot H_2O$	Violet	1620vs (br)	90	45.4 (45.2)	6.05 (6.3)	11.8 (11.7)
5 $[NMe_4]_2[CuL^2]\cdot H_2O$	Pink	1603vs (br)	85	46.0 (46.5)	6.8 (6.8)	14.6 (14.3)
6 $[NMe_4]_2[CuL^3]\cdot H_2O$	Red	1600s (br), 1582vs	85	47.9 (47.65)	6.6 (7.2)	16.6 (16.7)
7 $[PPh_4]_2[CuL^1]\cdot H_2O$	Violet	1647s, 1620vs	95	69.6 (69.1)	4.6 (4.6)	3.0 (2.8)
8 $[PPh_4]_2[CuL^2]\cdot 4H_2O$	Pink	1641m, 1603vs	90	65.5 (65.9)	4.8 (5.15)	3.7 (3.9)
9 $[PPh_4]_2[CuL^3]\cdot 5H_2O$	Red	1602s, 1580vs	90	65.0 (65.1)	5.4 (5.5)	5.1 (5.1)
10 $[PPh_4][CuL^3]\cdot MeCN$	Brown-black	1656vs, 1629s	45	62.0 (62.0)	4.7 (4.8)	9.7 (9.5)

[a] Required values are given in parentheses. [b] In KBr.

Table 2 Selected bond lengths (Å) and interbond angles (°)* for $[PPh_4][CuL^3]\cdot MeCN$ **10**

Copper environment			
Cu–N(1)	1.845(4)	Cu–N(3)	1.879(4)
Cu–N(2)	1.881(4)	Cu–N(4)	1.844(4)
N(1)–Cu–N(2)	85.0(2)	N(2)–Cu–N(3)	106.0(2)
N(1)–Cu–N(3)	168.7(2)	N(2)–Cu–N(4)	168.3(3)
N(1)–Cu–N(4)	84.3(2)	N(3)–Cu–N(4)	84.9(2)
L^3			
C(1)–O(1)	1.221(7)	C(2)–O(2)	1.232(7)
C(3)–O(3)	1.231(7)	C(4)–O(4)	1.233(7)
C(1)–N(1)	1.347(7)	C(2)–N(2)	1.334(7)
C(3)–N(3)	1.343(7)	C(4)–N(4)	1.348(7)
C(5)–N(1)	1.398(6)	C(6)–N(4)	1.405(6)
C(11)–N(2)	1.457(6)	C(12)–N(3)	1.460(6)
C(1)–C(2)	1.523(7)	C(3)–C(4)	1.519(7)
O(1)–C(1)–N(1)	126.0(5)	O(3)–C(3)–N(3)	125.9(5)
O(2)–C(2)–N(2)	126.6(4)	O(4)–C(4)–N(4)	126.1(5)
O(1)–C(1)–C(2)	123.8(5)	O(3)–C(3)–C(4)	121.2(5)
O(2)–C(2)–C(1)	120.0(5)	O(4)–C(4)–C(3)	123.3(5)
N(1)–C(1)–C(2)	110.2(4)	N(3)–C(3)–C(4)	112.8(4)
N(2)–C(2)–C(1)	113.3(4)	N(4)–C(4)–C(3)	110.6(4)
C(1)–N(1)–C(5)	127.7(4)	C(3)–N(3)–C(12)	118.2(4)
C(2)–N(2)–C(11)	117.2(4)	C(4)–N(4)–C(6)	128.0(4)
N(1)–C(5)–C(6)	112.7(4)	N(4)–C(6)–C(5)	112.2(4)
N(1)–C(5)–C(10)	127.4(5)	N(4)–C(6)–C(7)	127.6(5)

* Estimated standard deviations in the last significant digits are given in parentheses.

$\Delta\rho = -0.306$ e Å^{-3}; f, f' and f'' taken from the literature.[16] All calculations were performed by using SHELXS 86,[17] SHELX 76[18] and ORTEP[19] programs. Selected bond distances and angles are listed in Table 2.

Atomic coordinates, thermal parameters, and bond lengths and angles have been deposited at the Cambridge Crystallographic Data Centre (CCDC). See Instructions for Authors, *J. Chem. Soc.*, *Dalton Trans.*, 1997, Issue 1. Any request to the CCDC for this material should quote the full literature citation and the reference number 186/365.

Results and Discussion

Structure of complex 10

The crystal structure of $[PPh_4][CuL^3]\cdot MeCN$ **10** consists of discrete monomeric copper complex anions, $[CuL^3]^-$, tetraphenylphosphonium cations, and acetonitrile molecules of crystallization. A perspective view of the mononuclear anionic entity with the atom-numbering scheme is depicted in Fig. 1(*a*).

The copper atom is co-ordinated to the four deprotonated-amido nitrogen atoms of the chelating ligand in a nearly square-planar geometry. The Cu–N (amide) bond distances lie

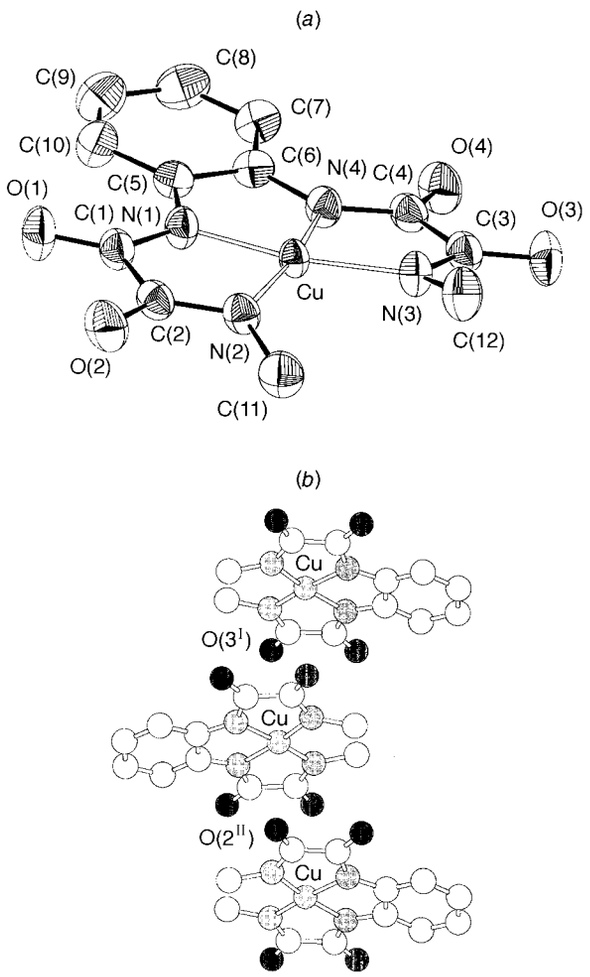

Fig. 1 (*a*) Perspective view of the anionic mononuclear unit of $[PPh_4][CuL^3]\cdot MeCN$ **10** with the atom-numbering scheme. Thermal ellipsoids are drawn at the 30% probability level; hydrogen atoms have been omitted for clarity. (*b*) Crystal packing diagram viewed down the *c* axis of the unit cell

in the range 1.84–1.88 Å, being significantly shorter than those of the analogous bonds to copper(II) (1.93–1.96 Å),[7] and similar to those observed in other copper(III) complexes containing bonds to amido nitrogens.[8–10] The shrinking of the metal–nitrogen bonds for Cu^{III} compared to Cu^{II} is a unique feature of this class of complexes. It is due to the diminution of the ionic radius on going from a di- to a tri-valent metal ion and enhanced by the relative gain in crystal-field stabilization of the low-spin d^8 over the d^9 electronic configurations in a square-planar co-ordination geometry. The same phenomenon can be

observed for the isoelectronic nickel(II) ion; M–N (amide) bond distances for low-spin d^8 nickel(II) square-planar complexes are shorter than those of high-spin d^8 octahedral ones (average 1.88 and 1.97 Å, respectively).[7b,20,21] Therefore, the metal–nitrogen bond lengths decrease in the order Ni^{II} (O_h) > Cu^{II} (D_{4h}) ≫ Ni^{II} (D_{4h}) > Cu^{III} (D_{4h}), as expected on the basis of the crystal-field stabilization effects.

The deprotonated L^3 forms three five-membered chelate rings around the metal ion with N (amide)–Cu–N (amide) bond angles in the range 84.3–85.0°, values which are close to 90° corresponding to the ideal square-planar geometry. The four nitrogen donor atoms around the copper are practically coplanar; two of them, N(1) and N(3), are above their least-squares plane by 0.063 and 0.051 Å, respectively, while the other two, N(2) and N(4), are approximately the same height below this plane (0.056 and 0.067 Å, respectively). The ruffling of the N_4 co-ordination scheme around the copper(III) ion results in a slight tetrahedral distortion from planarity, as in the related tripeptidecopper(III) complex of tri-α-aminoisobutyric acid (average value 0.05 Å)[9] and the *o*-phenylenebis(biuretato)copper(III) complex (0.12 Å).[8] The 6-5-6-membered chelate ring system of the *o*-phenylenebis-(biuretate) [*o*-$C_6H_4(NCONHCONH)_2$] ligand may contribute to the larger magnitude of the tetrahedral distortion compared to that found in the 5-5-5-membered ring systems of the tri-α-aminoisobutyrato and present copper(III) complexes, contrary to that reported previously for oxamidocopper(II) complexes.[7]

The entire L^3 ligand backbone is quasi-planar, with bond distances close to those found for the L^1 ligand in the copper(II) complex $[Ru(bipy)_3][CuL^1]\cdot 9H_2O$ (bipy = 2,2′-bypridine).[22] The observed C–N distances from the aromatic ring to N(1) and N(4) are those of single bonds, in this case close to 1.4 Å (1.40 and 1.41 Å, respectively). Moreover, the six C–C bond lengths in the aromatic ring are almost equivalent (average 1.39 Å), reflecting complete π delocalization within the aromatic ring. All these features are evidence against any ligand-centred oxidation consistent with a semiquinone-like ligand (*i.e.* L^3 is a 'redox innocent' ligand)[10] and, hence, unambiguously confirm a copper(III) formulation. Interestingly, within the oxamido fragment the C=O bonds decrease (average 1.23 Å) while the C–N ones lengthen (average 1.34 Å) when compared to those of analogous copper(II) complexes.[7,22] This reflects more double-bond character for the carbonyl group in complex **10**, as has been shown for the other copper(III) complexes reported.[8–10] Also, significant deviations from the least-squares plane formed by atoms Cu, N(1), N(2), N(3) and N(4) are seen for C(11) and C(12) belonging to the methyl groups. The approximately equal displacement of the methyl groups above and below the least-squares plane, 0.449 and 0.339 Å, respectively, probably reflects the presence of steric constraints between them. In this sense, this effect can contribute to the very slight tetrahedral distortion from planarity of the copper(III) centre, as described above.

The closest distances for possible axial interaction with copper(III) are 3.128 and 3.285 Å for the oxygen atoms O(3^I) (I $\frac{1}{2}+x, \frac{1}{2}-y, z$) and O($2^{II}$) (II $-\frac{1}{2}+x, \frac{1}{2}-y, z$) from adjacent molecules, respectively, which are however not reasonable bonding distances. These two non-bonded axial interactions can be seen very nicely in Fig. 1(*b*) which shows the packing diagram viewed down the *c* axis of the unit cell. Both of the Cu···O lines are practically perpendicular to the plane of the four Cu–N bonds, such that adjacent complexes are stacked almost parallel to each other. The angle between the mean basal planes of the copper atoms from two neighbouring units is 4.4°. Thus, the copper in this structure is strictly four-co-ordinated as found for all copper(III) complexes reported to date.[8–14] There is, however, one case of a five-co-ordinated copper(III) complex with a distorted square-pyramidal geometry. The copper is co-ordinated to a macrocyclic nitrogen-donor ligand with the fifth apical position being occupied by an oxygen atom from a hydroxo group (Cu–O 2.74 Å).[11] Apical co-ordination is frequently observed in oxamidatocopper(II) complexes [Cu–O(H_2O) 2.23–2.29 Å],[7f,g] whereas oxamidatonickel(II) complexes are usually square-planar diamagnetic species owing to the presence of strong-field amide nitrogen atoms within the co-ordination sphere. The axial Cu–O bond length in the above-mentioned square-pyramidal copper(III) complex is longer than the corresponding Ni–O (H_2O) bond lengths for the only octahedral nickel(II)–oxamide complex reported (average 2.12 Å).[7b]

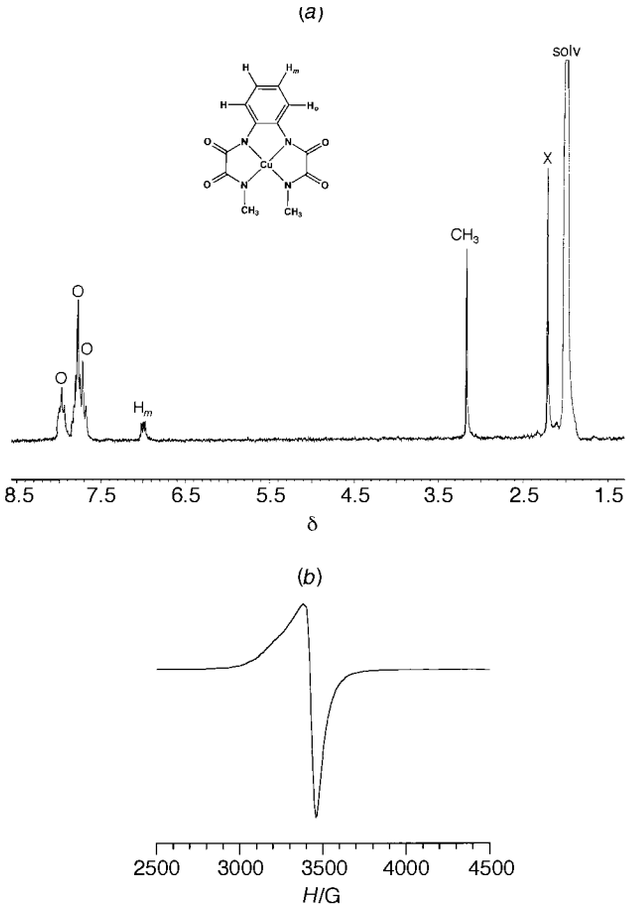

Fig. 2 (*a*) ^{1}H NMR spectrum of the copper(III) complex **10** in CD_3CN at room temperature (solv = solvent, o = tetraphenylphosphonium cation, X = impurity) and (*b*) the powder ESR spectrum of copper(II) complex **3** at room temperature; G = 10^{-4} T

Spectroscopic properties

^{1}H NMR and ESR. The ^{1}H NMR spectrum of complex **10** obtained in deuteriated acetonitrile is shown in Fig. 2(*a*). The signal assignment was simply deduced on comparison with the ^{1}H NMR spectrum of the free oxamide. The sharp singlet at δ 3.16 is attributed to the *N*-methyl protons of the tetradentate L^3 ligand (δ 2.73 for free L^3). The presence of only one double doublet at δ 7.00 associated with the *m*-proton of the benzene ring (δ 7.29 for free L^3) instead of two probably suggests that the *o*-proton signal is masked by the strong signals from the aromatic protons of the tetraphenylphosphonium cation located in the low-field region δ 7.6–8.1.† Both the sharpness of the NMR peaks as well as their almost negligible chemical shift compared to those of free L^3 are indicative of a diamagnetic

† This hypothesis is based on a comparison with the ^{1}H NMR spectrum of the isoelectronic diamagnetic nickel(II) complex $[PPh_4]_2[NiL^3]\cdot 5H_2O$, which shows the expected two double doublets at δ 6.54 and 8.01 derived from the two sets of *m*- and *o*-protons, respectively. The resonance corresponding to the *N*-methyl protons appears at δ 3.11 in this case.

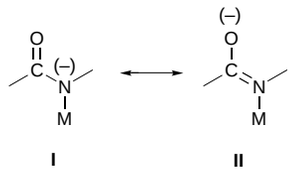

I II

copper(III) complex and, hence, a low-spin d^8 electronic configuration for Cu^{III}.

The diamagnetism of complex **10** is also reflected in its ESR-silent spectrum, in contrast to the paramagnetic copper(II) complexes. For instance, the related copper(II)–L^3 complex **3** shows an ESR spectrum typical of a d^9 copper(II) electronic configuration in axial symmetry as illustrated in Fig. 2(*b*), with $g_{\|}$ and $g_{\perp}$ values equal to 2.17 and 2.05, respectively. The corresponding *g* values for the other two copper(II) complexes of the series are $g_{\|} = 2.16$ and $g_{\perp} = 2.06$ for **1** and $g_{\|} = 2.17$ and $g_{\perp} = 2.06$ for **2**, thus revealing a tetragonal environment of the Cu^{II} for all these complexes.

Infrared and electronic. The most relevant CO absorption bands for the copper complexes **1**–**10** are listed in Table 1. Within the divalent metal series, the asymmetric C=O resonance frequency, corresponding to the average of the two vibrational modes ν_1(CO) and ν_7(CO) according to the literature,[23] are red shifted following the sequence $L^1 > L^2 > L^3$ [*e.g.* for the copper(II) tetraphenylphosphonium salts **7**–**9** where both bands are clearly shown], in line with the expected trend as the oxamato moieties are replaced by oxamido ones.[7b]

Furthermore, noticeable shifts are observed for the infrared frequencies of the C=O amide group from protonated H_4L^3 ligand to the copper(II)– and copper(III)–L^3 complexes, reflecting the different extents of π delocalization of the carbonyl double bond of the NCO amide fragment for each species. These observations are in accord with a weakening of the double-bond character of the C=O moiety and a more pronounced double-bond character of the C−N bond due to the increased contribution of resonance form **II** upon substitution of an amide proton by a metal ion (*i.e.* lower energy C=O frequencies for the metal complexes).[7] As discussed above, stronger Cu−N bonds are noted for the copper(III) when compared to those of the copper(II) complex, suggesting that delocalization of the excess of electron density resident on the deprotonated nitrogen in the NCO amido group is rendered more difficult in this case. That being so, resonance form **I** would be favoured thereby conferring less double-bond character to the C−N bond and a more double-bond character to the C−O bond as is experimentally found [*i.e.* the C=O frequencies for the copper(III) complex are intermediate between those of the copper(II) complex and of the pro-ligand].‡ Interestingly, from this peculiar difference in the infrared spectra between copper-(II) and -(III) complexes, Steggerda and co-workers[4] concluded that the metal in the compound obtained by electrolytic oxidation of the bis(oxamidato)copper(II) complex was effectively in the trivalent oxidation state, even when no structural evidence was available at that time.

The electronic absorption spectrum of the copper(III) complex **10** in acetonitrile is shown in Fig. 3, and compared to that of the corresponding copper(II) complex **9** [curves (*d*) and (*c*), respectively]. It consists of an intense band in the UV region centred at 340 nm, with three distinct shoulders which extend

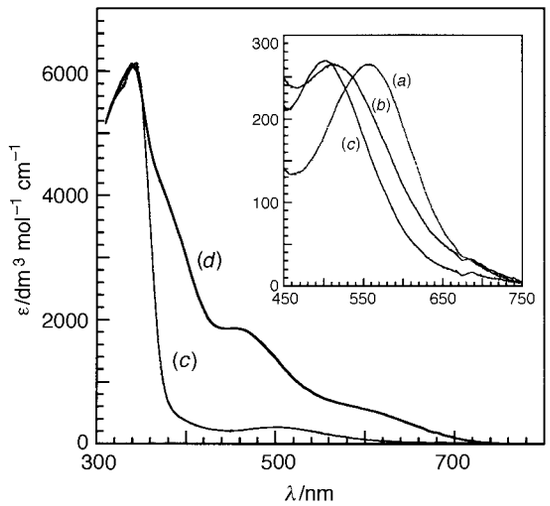

Fig. 3 Electronic absorption spectra of the copper(II) complexes **7**–**9** [curves (*a*)–(*c*)] and the copper(III) complex **10** (*d*) in acetonitrile

into the visible region located at 380, 460 and 600 nm, respectively. The high-energy peak, which also appears in the spectrum of the copper(II) complex as a single band with almost the same location and intensity, is commonly assigned to the π–π* transition within the aromatic ring of the ligand, while the weak shoulders on the low-energy tail of this intraligand absorption band may then originate from d–d transitions. For a diamagnetic copper(III) ion with a d^8 electronic configuration in a square-planar environment three transitions are expected. These correspond to the individual transitions from the four lower-lying fully occupied d orbitals to the upper empty d orbital (*i.e.* $^1A_{1g} \longrightarrow {}^1B_{1g}$, $^1A_{1g} \longrightarrow {}^1A_{2g}$ and $^1A_{1g} \longrightarrow {}^1E_{1g}$ transitions in D_{4h} symmetry).[24] However, it is not possible to determine unequivocally the assignment of these transitions because the energy order of the lower four d orbitals is not known. The four lower d orbitals are often so close together in energy that individual transitions therefrom to the upper d level cannot be distinguished. This is the case for example for the isoelectronic yellow nickel(II) complex $[PPh_4]_2[NiL^3]\cdot 5H_2O$, which shows a single shoulder on the low-energy tail of the intraligand absorption band at *ca.* 420 nm.

The electronic absorption spectra of acetonitrile solutions of the copper(II) complexes **7**–**9** show a similar pattern consisting of the above-mentioned intraligand band in the UV region, at *ca.* 340 nm, with a second less intense band in the visible region, the location of which varies over the narrow range 560–500 nm depending upon the nature of the copper(II) complex, *i.e.* at 560, 520 and 500 nm, respectively [curves (*a*)–(*c*) in the insert of Fig. 3]. This low-energy band is the typical d–d transition band of Cu^{II} in a square-planar environment which actually envelopes three d–d transitions (*i.e.* $^2B_{1g} \longrightarrow {}^2A_{1g}$, $^2B_{1g} \longrightarrow {}^2B_{2g}$ and $^2B_{1g} \longrightarrow {}^2E_{1g}$ in D_{4h} symmetry).[24] If the relative positions and intensities of these three transitions remain constant, the position of the maximum for the band envelope is a measure of the ligand-field strength and, hence, indicative of the crystal-field stabilization energy (c.f.s.e.). So, the observed blue shift in the visible absorption maxima along this series of copper(II) complexes is in agreement with the stronger ligand field associated with nitrogen-donor ligands rather than oxygen ones, *e.g.* the CuN_2O_2 chromophore for $[CuL^1]^{2-}$, CuN_3O for $[CuL^2]^{2-}$ and CuN_4 for $[CuL^3]^{2-}$. This ligand-field effect merely reflects a stronger metal–ligand σ-bonding destabilization of the singly occupied highest occupied molecular orbital of the copper(II) complex, as will be evidenced from the electrochemical behaviour.

Electrochemical study

The electrochemical behaviour of this series of copper com-

‡ This correlation between the position of the CO amide absorption bands and the metal–nitrogen (amido) bond lengths is further confirmed by the nickel(II) complex $[PPh_4]_2[NiL^3]\cdot 5H_2O$, which also shows two strong ν(CO) bands at 1616 and 1590 cm^{-1}, *i.e.* intermediate between those of the corresponding copper(II)– and copper(III)–L^3 complexes (see Table 1). The metal–nitrogen bond lengths decrease in the order $Cu^{II} \gg Ni^{II} > Cu^{III}$ along this series of square-planar complexes as mentioned in the structural discussion.

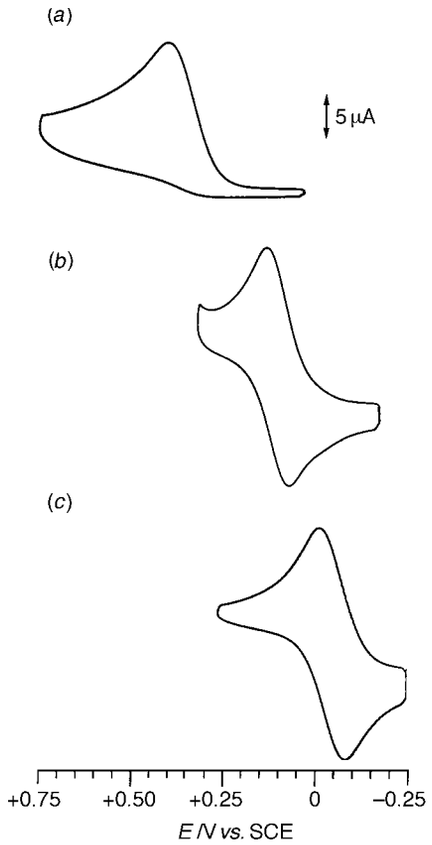

Fig. 4 Cyclic voltammograms for (*a*) $[CuL^1]^{-/2-}$, (*b*) $[CuL^2]^{-/2-}$ and (*c*) $[CuL^3]^{-/2-}$ couples in acetonitrile at 25 °C

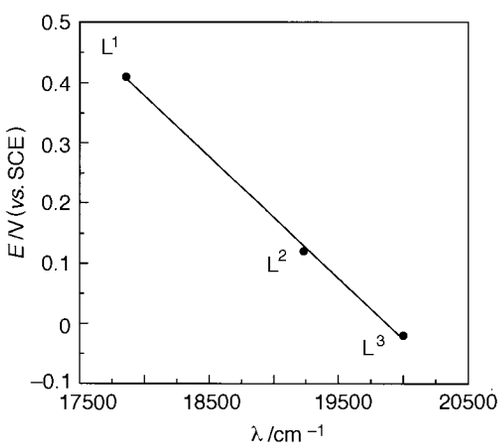

Fig. 5 The Cu^{III}–Cu^{II} redox potentials as a function of the copper(II) d–d absorption maxima

plexes is illustrated in Fig. 4, which shows the voltammograms of the copper(II) complexes **4**–**6** in acetonitrile [curves (*a*)–(*c*), respectively]. All the copper(II) compounds undergo one-electron oxidation in the potential range 0.41 to −0.02 V *vs.* SCE, all of them being reversible except for the former, where no reverse reduction peak is detected even at high scan rates, revealing that a fast chemical reaction is coupled to the electrochemical process in that case. This reaction is tentatively assigned to a copper(III)-catalysed hydrolytic decomposition of the oxamate ligand L^1 yielding the corresponding oxalato complexes. Actually, hydrolysis of amides proceeds by nucleophilic attack of H_2O (or OH^- in basic medium) on the amide group carbon atom. Since higher-valent metal ions are much more polarizing, substituting a copper-(III) for a -(II) ion increases the positive charge density on the amide carbon and thus increases its susceptibility to nucleophilic attack.[7d]

The shift in the formal potentials of the copper(III)–copper(II) couples to more negative values, *i.e.* stabilizing the higher oxidation state, which occurs upon ligand substitution along this series can be attributed to the greater donor capacity (basicity) of the deprotonated-amido nitrogen atoms compared to that of the carboxylate oxygen ones. Hence, the electron density at the metal centre is enhanced as the number of the N-amido donor groups is increased, thus facilitating its oxidation. Moreover, the resulting copper(III) complex is stabilized towards hydrolytic decomposition, thus enabling its isolation. The $[CuL^2]^{2-}$ complex has three deprotonated-amido nitrogens and a carboxylate oxygen bound to the metal. The Cu^{III}–Cu^{II} potential is lowered by 290 mV (0.12 V) compared to the $[CuL^1]^{2-}$ complex (0.41 V), which contains two deprotonated-amido nitrogens and two carboxylate oxygen donor atoms. However, replacement of another carboxylate group by an amido function in the complex $[CuL^3]^{2-}$, thus providing an environment of four deprotonated-amido nitrogens bound to the metal, induces a change of only 100 mV (−0.02 V) in the Cu^{III}–Cu^{II} potential, as compared to that of $[CuL^2]^{2-}$. This disappointing behaviour may be explained by the slight distortion of the planar environment of copper(III) in the $[CuL^3]^-$ moiety owing to the steric hindrance between neighbouring methyl groups, as revealed by the structure of **10**. Consequently, a decrease in the overall stability of the copper(III) complex is expected, which would result in an increase in the Cu^{III}–Cu^{II} potential, as is confirmed by experience.

It is to be noted that the energy values of the visible absorption maxima for the copper(II) complexes increase in a non-linear monotonic fashion with the number of amido groups along this series, suggesting that a similar distortion of the planar environment of the metal is also operative in the Cu^{II}–L^2 complex. Furthermore, there is a perfect correlation between the Cu^{III}–Cu^{II} redox potentials and the visible absorption maxima of the copper(II) complexes, as illustrated in Fig. 5. The same phenomenon has been previously observed by Margerum and co-workers[25] in an exhaustive study involving a large number of copper(II)–peptide complexes. They concluded that this correlation merely reflects the relative gain in the c.f.s.e. for the change from d^9 Cu^{II} (square planar) to d^8 Cu^{III} (low-spin, square planar). This stabilization energy is estimated to be *ca.* 15/12 *Dq* when going from a d^9 electronic configuration in square-planar geometry (13/12 *Dq*) to a low-spin d^8 electronic configuration (28/12 *Dq*), to which the further effect due to the increase in the value of *Dq* for the change of a di- to a trivalent ion is to be added.§ Then, any factor which increases the c.f.s.e. for the copper(II) complexes causes an even greater increase for the copper(III) complexes and, therefore, results in a shift of the formal potentials of the copper(III)–copper(II) couples to more negative values thereby stabilizing the copper(III) oxidation state.

In summary, it can be concluded that the selective stabilization of this rather high oxidation state of copper in complex **10** is rendered possible by the strong electron-donating ability of the deprotonated-amide nitrogen atoms and the near square-planar co-ordination afforded by the disubstituted oxamide ligands. This effect was first clearly demonstrated by Margerum and co-workers[25] for copper–peptide complexes. In this respect,

§ The complex $[NMe_4]_2[NiL^3]\cdot 4H_2O$ undergoes a reversible one-electron redox process under the same conditions with a formal potential for the nickel(III)–nickel(II) couple equal to 0.13 V (*vs.* SCE), *i.e.* 150 mV higher than the corresponding copper(II)–L^3 complex (−0.02 V). However, the attainment of the trivalent state for the copper complex is expected to be much more difficult, essentially owing to the larger value of its third ionization energy compared to that of nickel. This anomalous behaviour shows again the greater gain in c.f.s.e. in a square-planar environment for the Cu^{II}–Cu^{III} redox change with respect to the Ni^{II}–Ni^{III} process. The change from low-spin d^8 Ni^{II} to low-spin d^7 Ni^{III} involves a stabilization in terms of c.f.s.e. of only 3/12 *Dq*, which is a relatively smaller energy gain compared to that of copper, *i.e.* 15/12 *Dq*.

Table 3 The Cu^{III}–Cu^{II} redox potentials (*vs.* SCE) for complexes of a related class of *o*-phenylenebis(amide) ligands

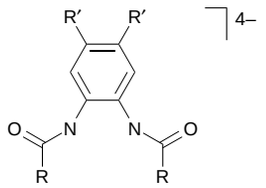

R	R′	E/V
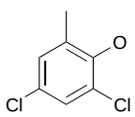	Cl	0.51[a]
	H	0.41[b]
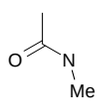	H	–0.02[b]
	Cl	–0.44[a]
	H	–0.47[a]

[a] Ref. 10. [b] This work.

the formal potential values for the copper compounds investigated herein are intermediate between those found by Collins and co-workers[10] corresponding to diphenoxo- and dialkoxo-substituted compounds, as illustrated in Table 3. Then, the trend in the donor capacity of each co-ordinating group is as follows: phenoxo < carboxylate < amido < alkoxo. Extension of this work to other transition-metal ions with unusually high oxidation states is in progress in our laboratory.

Acknowledgements

We thank Dr. J. Sainton for recording the ^{1}H NMR spectra. Financial support from the Direccion General de Investigación Científica y Técnica (DGICYT) (Spain) through Project PB91-0807-002-01 and the Human Capital and Mobility Program (Network on Magnetic Molecular Materials from EECC) through grant ERBCHRXCT920080 is gratefully acknowledged. R. R. and J. C. thank the Ministerio de Educación y Ciencia (Spain) for post- and pre-doctoral grants, respectively.

References

1 T. F. Collins, *Acc. Chem. Res.*, 1994, **27**, 279 and refs. therein.
2 K. Nag and A. Chakravorty, *Coord. Chem. Rev.*, 1980, **33**, 87.
3 H. Sigel and R. B. Martin, *Chem. Rev.*, 1982, **82**, 385.
4 J. J. Bour, P. J. M. W. L. Birker and J. J. Steggerda, *Inorg. Chem.*, 1971, **10**, 1202.
5 H. Ojima and K. Nonoyama, *Coord. Chem. Rev.*, 1988, **92**, 85.
6 R. Ruiz, Ph.D. Thesis, University of Valencia, 1995.
7 (*a*) F. Lloret, M. Julve, J. Faus, Y. Journaux, M. Philoche-Levisalles and Y. Jeannin, *Inorg. Chem.*, 1989, **28**, 3702; (*b*) F. Lloret, J. Sletten, R. Ruiz, M. Julve, J. Faus and M. Verdaguer, *Inorg. Chem.*, 1992, **31**, 779; (*c*) F. Lloret, M. Julve, J. Faus, R. Ruiz, I. Castro, M. Mollar and M. Philoche-Levisalles, *Inorg. Chem.*, 1992, **31**, 784; (*d*) J. Soto, R. Martinez-Mañez, J. Paya, F. Lloret and M. Julve, *Transition Met. Chem.*, 1993, **18**, 69; (*e*) F. Lloret, M. Julve, J. A. Real, J. Faus, R. Ruiz, M. Mollar, I. Castro and C. Bois, *Inorg. Chem.*, 1992, **31**, 2956; (*f*) J. A. Real, M. Mollar, R. Ruiz, J. Faus, F. Lloret, M. Julve and M. Philoche-Levisalles, *J. Chem. Soc., Dalton Trans.*, 1993, 1483; (*g*) J. A. Real, R. Ruiz, J. Faus, F. Lloret, M. Julve, Y. Journaux, M. Philoche-Levisalles and C. Bois, *J. Chem. Soc., Dalton Trans.*, 1994, 3769; (*h*) J. L. Sanz, B. Cervera, R. Ruiz, C. Bois, J. Faus, F. Lloret and M. Julve, *J. Chem. Soc., Dalton Trans.*, 1996, 1359.
8 P. J. M. W. L. Birker, *J. Chem. Soc., Chem. Commun.*, 1977, 444.
9 L. L. Diaddario, W. R. Robinson and D. W. Margerum, *Inorg. Chem.*, 1983, **22**, 1021.
10 F. C. Anson, T. J. Collins, T. G. Richmond, B. D. Santarsiero, J. E. Toth and B. G. R. T. Treco, *J. Am. Chem. Soc.*, 1987, **109**, 2974.
11 W. E. Keys, J. B. R. Dunn and T. M. J. Loehr, *J. Am. Chem. Soc.*, 1977, **99**, 4527.
12 B. R. Serr, C. E. L. Headford, C. M. Elliot and O. P. Anderson, *Acta Crystallogr., Sect. C*, 1990, **46**, 500.
13 M. R. Caira, K. R. Koch and C. Sacht, *Acta Crystallogr., Sect. C*, 1991, **47**, 26.
14 T. M. Yao, X. Z. You, C. Li, L. F. Li and Q. C. Yang, *Acta Crystallogr., Sect. C*, 1994, **50**, 67.
15 H. O. Stumpf, Y. Pei, O. Kahn, J. Sletten and J. P. Renard, *J. Am. Chem. Soc.*, 1993, **115**, 6738.
16 *International Tables for X-Ray Crystallography*, Kynoch Press, Birmingham, 1974, vol. 4, p. 99.
17 G. M. Sheldrick, SHELXS 86, A Program for Crystal Structure Determination, University of Göttingen, 1986.
18 G. M. Sheldrick, SHELX 76, A Computer Program for Crystal Structure Determination, University of Cambridge, 1976.
19 C. K. Johnson, ORTEP, Report ORNL-3794, Oak Ridge National Laboratory, Oak Ridge, TN, 1971.
20 A. C. Fabretti, A. Giusti, V. G. Albano, C. Castellani, D. Gatteschi and R. Sessoli, *J. Chem. Soc., Dalton Trans.*, 1991, 2133.
21 Z. N. Chen, W. X. Tang, J. Chen, P. J. Zheng, C. G. Chen and K. B. Yu, *Polyhedron*, 1994, **13**, 873.
22 S. S. Turner, C. Michaut, O. Kahn, L. Ouahab, A. Lecas and E. Amouyal, *New J. Chem.*, 1995, **19**, 773.
23 K. Nakamoto, *Infrared and Raman Spectra of Inorganic and Coordination Compounds*, Wiley, New York, 4th edn., 1986, ch. 3, p. 244.
24 Y. Nishida and S. Kida, *Coord. Chem. Rev.*, 1979, **27**, 275.
25 F. P. Bossu, K. L. Chellapa and D. W. Margerum, *J. Am. Chem. Soc.*, 1977, **99**, 2195.

Received 6*th November* 1996; *Paper* 6/07572J